Int. J. Heat Mass Transfer. Vol. 16, pp. 1245–1265. Pergamon Press 1973. Printed in Great Britain

NATURAL CONVECTION IN A SOUND FIELD GIVING LARGE STREAMING REYNOLDS NUMBERS

G. DE VAHL DAVIS* and P. D. RICHARDSON
Division of Engineering, Brown University, Providence, R.I. 02912, U.S.A.

(*Received* 28 *April* 1972 *and in revised form* 23 *October* 1972)

Abstract— Natural convection around a horizontal circular isothermal cylinder is considered in conjunction with a transverse standing sound field propagated in the vertical or the horizontal direction. The problem is treated within the framework of boundary-layer theory with the formulation including creation or modification of the steady convective motion by the Reynolds stresses associated with the oscillations. Results are presented for a range of parameters expressing boundary layer quantities and oscillation magnitudes for $Pr = 0{\cdot}7$ and $2{\cdot}85$. Horizontal oscillations increase heat transfer at the bottom of a cylinder, and vertical oscillations decrease the local heat transfer; when the intensity of vertical oscillations is large enough, a region of reversed flow develops; corresponding effects have been observed in experiments.

1. INTRODUCTION

AMONG the methods which have been proposed for achieving an economical increase in convective heat transfer rates from a surface, the use of oscillations in the fluid or vibrations of the surface has received considerable attention. Many experiments have been reported, with most results indicating an increase in heat transfer due to oscillations or vibrations. Until very recently there was no analysis which successfully accounted for any of the measurements on a satisfactory, fluid-mechanical basis. It is not expected that a single method of analysis will be adequate to explain all reported measurements, since there is strong evidence of effects in both laminar and turbulent flows, which usually must be considered separately. A review of the subject was presented recently [1].

Richardson [2] considered the extensive measurements available for heat transfer from a horizontal heated cylinder which is supported in a transverse sound field or mechanically vibrated transverse to its axis. He presented an analysis of the problem in which buoyancy forces were ignored, and found favorable comparison with experimental results, especially when the influence of buoyancy on the steady motion generated by the oscillations was small ($Gr/Re^2 \to 0$).

It is the purpose of this paper to present an analysis in which the influence of buoyancy is restored, and to give some illustrative solutions. These solutions are obtained from the coupled momentum and energy equations, and are valid in a region near the lower stagnation point of the cylinder. Before giving details of the analysis, it is important to discuss the physical background for it.

Attention is restricted here to sound fields and vibrations for which the corresponding acoustic wavelength is large compared with the cylinder diameter. It is then possible to consider the fluid in the neighborhood of the cylinder as incompressible; for this case it is immaterial whether the fluid is stationary and cylinder oscillating or vice versa. This remains true if a density variation occurs only in buoyancy terms of the equations, i.e. if the Boussinesq approximation is made.

* On leave from the University of New South Wales, Kensington, Australia.

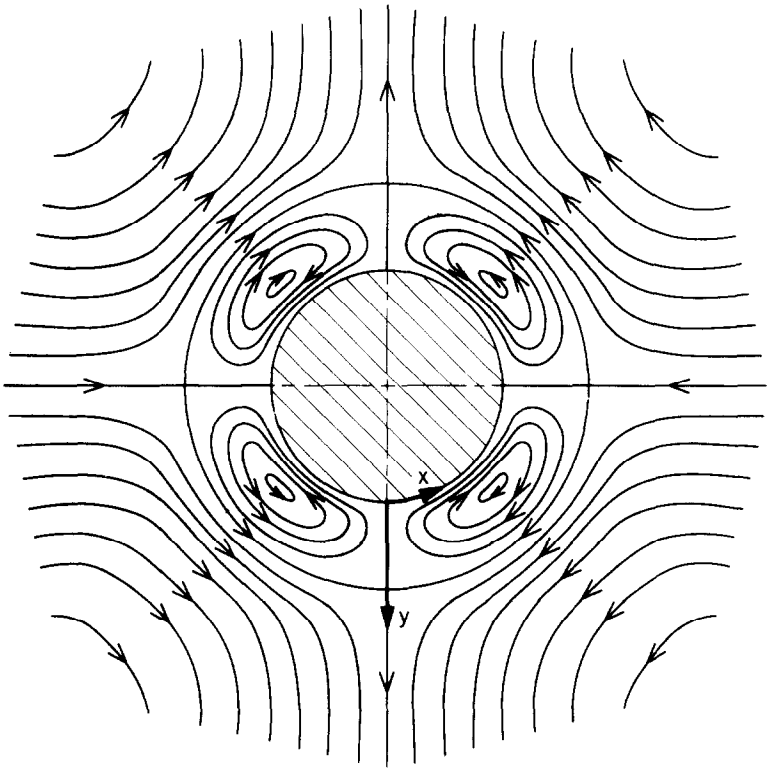

FIG. 1. Isothermal acoustic streaming around a circular cylinder at small streaming Reynolds numbers.

Isothermal, harmonic free-stream oscillations in a fluid surrounding a stationary cylinder give rise to a steady motion near the cylinder, known as acoustic streaming [3]. This motion is illustrated in Fig. 1 and consists of two parts. In each quadrant a circulatory motion is established. For horizontal oscillations (as shown) the motion near the surface is from the equator to the poles. Radially beyond this region the motion is in the opposite direction. The outer flow depends upon the streaming Reynolds number, $a^2\omega/\nu$; for small values of this parameter, the outermost motion is as illustrated with flows towards and away from the cylinder along vertical and horizontal planes, while for large values of the parameter the velocities in the outer flow are reduced and the approaching flow is more evenly distributed over the circumference of the cylinder, although the plane jets of outflow remain [4].

When the flow around the cylinder is not isothermal, the streaming motion is affected. A variation in the local acoustic impedance (ρ times the speed of sound) occurs through the thermal boundary layer, and this alters the Reynolds stresses—which drive the streaming motion—in a way that is complicated to analyse. Clearly, the general case involves a complicated coupling between the momentum and energy equations. The temperature distribution is determined from the energy equation in which the coefficients include the streaming velocity components. These velocity components, in turn, are determined from the momentum equation

for the time-averaged flow for which the driving stresses are derived from the temperature field (through the buoyancy term) and from the primary oscillating flow. The local velocity components for the latter flow are affected by the complete impedance field. The same coupling is found in ordinary convection problems, and it is usually necessary to introduce simplifying assumptions to make the equations tractable. In incompressible flow the fluid properties are often assumed constant. Comparison with experiment is good unless very large property variations are involved. It is encouraging that Richardson [2] found good comparison on this basis.

The convective motion near a horizontal heated cylinder in a gravitational field has been studied by Hermann [5], by Chiang and Kaye [6], and by Saville and Churchill [7]. The method of solution to be described here is an extension of that of Chiang and Kaye, the final equations being rather similar although their genesis is somewhat different. As pointed out by Churchill [8], a complete description of natural convection from a heated body immersed in an infinite fluid is difficult to achieve because of the problem of representing adequately the motion far from the body, where the fluid carried up by buoyancy must descend. A boundary layer approach is adopted here, and use of this method cannot be expected to yield useful information near to or downstream of the point of separation of flow from the surface. The method is therefore limited in its application to regions not too remote from the forward stagnation point of the flow (i.e. the lowest point on the circumference of the cylinder), and also to large streaming Reynolds numbers.

The diffusion of vorticity (periodically varying in sign) into the fluid occurs through a characteristic length scale, $(\nu/\omega)^{\frac{1}{2}}$, known as the a.c. boundary layer thickness. For boundary layer analysis to be applied, this thickness must be small compared with the cylinder radius. For example, in fluids such as water or air, with frequencies of 100 cps or more, the a.c. boundary layer is of the order of 10^{-3} ft or less. For all but the smallest cylinders, therefore, the boundary layer approach is easily justified as far as the oscillations are concerned. We wish to be able to use, as one boundary condition in the equations derived, that the steady (streaming) motion is vanishingly small at the edge of the thermal boundary layer. This requires that $a^2\omega/\nu$ is large, or that $R/Gr^{\frac{1}{4}}$ is large; but the latter condition implies that $Gr^{\frac{1}{4}}$ is small, which falls outside the scope of boundary layer analysis. The basic question is how to choose conditions such that results of analysis can be compared with existing experimental data or, if there are inadequate local transport data available, how to choose conditions such that suitable data might be forthcoming. Since the analysis starts from pure natural convection, for boundary layer analysis to be employed the thermal boundary layer must be fairly thin compared with the cylinder radius. The laminar thermal boundary layer thickness is of the order of $R/Gr^{\frac{1}{4}}$; for this to be smaller than, say, $R/10$ requires that Gr be greater than 10^4. The effects of oscillations appear to be stronger when the a.c. boundary layer thickness is small compared with the natural convection boundary layer thickness. And for $R/10$ to be large in comparison with an a.c. boundary layer thickness of 10^{-3} ft places a minimum of R of a few hundredths of a foot.

When the direction of oscillation of the cylinder, or of propagation of a sound field around the cylinder, is either vertical or horizontal, it is possible to obtain a similarity solution for the region of the flow in the neighborhood of the stagnation point on the bottom of the cylinder.

2. DERIVATION OF EQUATIONS

The equations of motion are most conveniently written in curvilinear coordinates, shown in Fig. 1, in which the origin is at the lower stagnation point, the x-axis lies along the surface and the y-axis is normal to it. This notation is standard for natural convection, but differs

from the usage of Richardson in analyzing heat transfer by acoustic streaming, where the z-axis was normal to the cylinder.

At large distances from the cylinder, the fluid possesses an oscillatory motion described by

$$U = U_\infty \cos \omega t. \tag{1}$$

Nearer the cylinder, but outside the oscillation boundary layer, the velocity component parallel to the surface is

$$U(x, t) = U_0(x) \cos \omega t, \text{ given by either}$$

$$U(x, t) = 2U_\infty \sin (x/R) \cos \omega t \tag{2a}$$

or

$$U(x, t) = 2U_\infty \cos (x/R) \cos \omega t \tag{2b}$$

depending upon whether the externally imposed oscillations are in a vertical or horizontal direction respectively.

In the curvilinear system, the boundary-layer equations retain their usual form provided the boundary-layer thickness is small in comparison with the radius of curvature of the surface, and the radius of curvature itself does not vary rapidly along the surface. In the present case, the latter condition is satisfied exactly ($dR/dx = 0$), while the former is acceptable in the vicinity of the origin.

Conservation of momentum in the x-direction is expressed by

$$\frac{\partial u}{\partial t} + u\frac{\partial u}{\partial x} + v\frac{\partial u}{\partial y} = -\frac{1}{\rho}\frac{\partial p}{\partial x} + \nu\frac{\partial^2 u}{\partial y^2} + g\beta(T - T_\infty)\sin(x/R)$$

or, since

$$-\frac{1}{\rho}\frac{\partial p}{\partial x} = \frac{\partial U}{\partial t} + U\frac{\partial U}{\partial x}$$

by

$$\frac{\partial u}{\partial t} - \nu\frac{\partial^2 u}{\partial y^2} - \frac{\partial U}{\partial t} = -u\frac{\partial u}{\partial x} - v\frac{\partial u}{\partial y} + U\frac{\partial U}{\partial x} + g\beta(T - T_\infty)\sin(x/R). \tag{3}$$

The equation has been written in this way because the terms on the left hand side are, for thin layers and high frequencies, of a larger order of magnitude than those on the right. The associated energy equation is, as usual,

$$u\frac{\partial T}{\partial x} + v\frac{\partial T}{\partial y} = \alpha\frac{\partial^2 T}{\partial y^2}. \tag{4}$$

A first approximation to the solution of (3) is found by setting the right hand terms to zero. Introducing a dimensionless wall distance $\eta = y(\omega/2\nu)^{\frac{1}{2}}$, the first approximation to the stream function is found to be

$$\psi = -\left(\frac{2\nu}{\omega}\right)^{\frac{1}{2}}\frac{U_0}{2}\{(1 - i) \times [1 - \exp(-(1 + i)\eta)] - 2\eta\}\exp(i\omega t).$$

The resulting velocity components are then

$$u = \frac{\partial \psi}{\partial y} = U_0\{\cos \omega t - \exp(-\eta) \times \cos(\omega t - \eta)\} \tag{5a}$$

$$v = -\frac{\partial \psi}{\partial x} = -\left(\frac{2\nu}{\omega}\right)^{\frac{1}{2}} U_0'\left\{\eta \cos \omega t + \frac{1}{\sqrt{2}}\cos(\omega t + 3\pi/4) + \frac{1}{\sqrt{2}}\exp(-\eta) \times \cos(\omega t - \eta - \pi/4)\right\}. \tag{5b}$$

These expressions may be inserted into equation (3) to yield a second approximation to the solution. Before doing so, however, we anticipate that the final velocities may contain both steady and fluctuating parts, and write, in (3),

$$u = \bar{u} + u', \qquad v = \bar{v} + v'.$$

When the time average of each term in (3) is then calculated, the equation for the mean motion is obtained:

$$\bar{u}\frac{\partial \bar{u}}{\partial x} + \bar{v}\frac{\partial \bar{u}}{\partial y} = \frac{U_0}{2}\frac{dU_0}{dx} + \nu\frac{\partial^2 \bar{u}}{\partial y^2} - \frac{\partial}{\partial x}\overline{u'^2} - \frac{\partial}{\partial y}\overline{u'v'} + g\beta\theta \sin x/R. \tag{6}$$

The terms containing u' and v' involve the Reynolds stresses, analogous to those which arise in turbulent flow. Here, however, the fluctuations are the result of the imposed oscillatory motion. We now assume that a solution of the complete equation (6)—the time-averaged version of (3)—can be obtained by using the approximate expressions $(5a + b)$ for u' and v'.

This leads to

$$\overline{u'^2} = U_0^2\{\tfrac{1}{2} - \exp(-\eta)\cos\eta + \tfrac{1}{2}\exp(-2\eta)\}$$

$$\overline{u'v'} = -\left(\frac{2\nu}{\omega}\right)^{\frac{1}{2}} U_0 U_0' \left\{\frac{\eta}{2} - \frac{1}{4} + \frac{\exp(-\eta)\cos n}{2} - \frac{\eta}{2}\exp(-\eta)\cos\eta - \frac{1}{4}\exp(-2\eta)\right\}$$

and hence

$$\frac{\partial}{\partial x}\overline{u'^2} = U_0 U_0'\{1 - 2\exp(-\eta)\cos\eta + \exp(-2\eta)\}$$

$$\frac{\partial}{\partial y}\overline{u'v'} = -U_0 U_0' \left\{\frac{1}{2} - \frac{1}{2}\exp(-\eta)\cos\eta + \frac{1}{\sqrt{2}}(\eta - 1)\exp(-\eta)\cos\left(\eta - \frac{\pi}{4}\right) + \frac{1}{2}\exp(-2\eta)\right\}.$$

We next introduce the following set of dimensionless variables*:

$$\xi = x/R;$$

$$E = Gr^{\frac{1}{2}} y/R = Gr^{\frac{1}{2}}(2\nu/\omega)^{\frac{1}{2}}\eta/R = \eta/\lambda \text{ say};$$

$$\psi = Gr^{\frac{1}{2}}\nu\xi F(E);$$

$$G = \theta/\theta_0 = (T - T_\infty)/(T_\omega - T_\infty).$$

Furthermore, since we are limiting our attention to small values of x, we may set $\sin(x/R) = x/R$. Equations (6) and (4) then become

$$F''' + F''\cdot F - F'^2 + G \pm Kf(\lambda E) = 0 \quad (7)$$

$$G'' + Pr\cdot G'\cdot F = 0 \quad (8)$$

where primes denote differentiation with respect to E, K denotes

$$\frac{4U_\infty^2 R^2}{Gr\,\nu^2},$$

the negative (positive) sign in (7) is taken for horizontal (vertical) oscillations in the far field, and $f(\lambda E)$ stands for

$$\frac{3}{2}\exp(-\lambda E)\cos\lambda E - \frac{1}{2}\exp(-2\lambda E) + \frac{1}{\sqrt{2}}\exp(-\lambda E)(\lambda E - 1)\cos(\lambda E - \pi/4).$$

A typical variation of $f(\lambda E)$ with E is shown in Fig. 2. The approach of $f(\lambda E)$ to its limiting value of zero is an indication of the diminishing effect on the motion of the oscillations which generate the Reynolds stresses.

The solution is seen to be dependent upon three parameters: K, λ and Pr. In the nomenclature used previously by Richardson [9],

$$K = s\,Re_{osc}^2/Gr,$$

where $Re_{osc} = 2^{\frac{1}{2}}U_\infty R/\nu$, and is known as the oscillation Reynolds number. Thus K expresses the intensity of the effects of oscillation in terms of the intensity of the buoyancy effects. The parameter λ can be written

$$\lambda = \frac{R/Gr^{\frac{1}{2}}}{2^{\frac{1}{2}}(\nu/\omega)^{\frac{1}{2}}},$$

and is a direct measure of the ratio of the thermal and a.c. boundary-layer thicknesses. When λ is large the a.c. boundary layer is very thin compared with the natural convection boundary layer.

The solution of (7) and (8) is not immediately dependent upon the Grashof number. However, the parameter of practical interest, the Nusselt number, is given by

$$Nu = \frac{hR}{k} = -Gr^{\frac{1}{2}}G'(0).$$

* These variables are not unique; for very small Prandtl numbers, or to compute directly the case $Gr = 0$, $Re_s \to \infty$, other sets of variables arise.

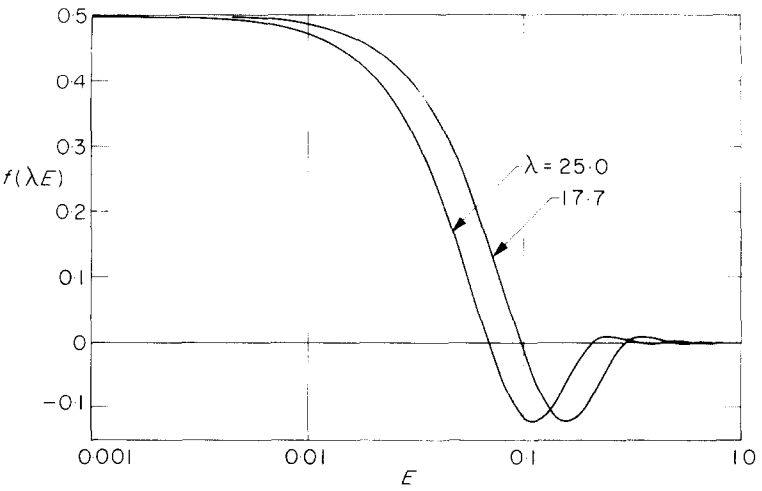

FIG. 2. The variable $f(\lambda E)$ as a function of E. It should be noted that the E scale is logarithmic.

Another parameter used by Richardson is a streaming strength parameter

$$\varepsilon = 4Re_s/Gr^{\frac{1}{2}},$$

where $Re_s = U_\infty^2/\omega\nu$, the streaming Reynolds number; Re_s is also given by $a^2\omega/\nu$, where a is the amplitude of oscillation; thus Re_s is the square of the ratio of this amplitude to the a.c. boundary-layer thickness. In terms of the present parameters,

$$\varepsilon = Re_{osc}^2/Gr\lambda^2 = K/2\lambda^2.$$

The boundary conditions to which (7) and (8) are subject are that the velocity shall vanish at the surface of the cylinder, the azimuthal velocity component shall vanish at large wall distances* and the temperature shall have specified values at the surface and far from it. In terms of the new variables, these boundary conditions are

$$\begin{aligned} &F = F' = 0, \quad G = 1 \quad \text{at} \quad E = 0, \\ &F' \to 0, \quad G \to 0 \quad \text{at} \quad E \to \infty. \end{aligned} \tag{9}$$

* It will be noticed that F' represents the azimuthal component of the *mean* velocity, and that (by application of the continuity equation) F is proportional to the normal component. As a result of the averaging process, the fluctuations do not appear in the boundary conditions.

The results of computations for the solutions of equations (7)–(9) display so many of the characteristics which have been observed qualitatively in experiment that it was decided to extend the solutions by using series expansions of $\sin(x/R)$ and $\cos(x/R)$ instead of the one-term approximations, valid as $x/R \to 0$, used in equations (7) and (8). These added terms give rise to modifications of the solutions of (7)–(9) in the azimuthal direction. However, these modifications are of magnitudes rather than of basic flow patterns and discussion of the extended solutions is deferred so that only the basic solutions are presented here.

3. COMPUTATIONAL PROCEDURE

Equations (7)–(9) represent a two-point boundary-value problem. Solution is rendered difficult because two boundary values are not known *a priori*—the values of F'' and G' at the wall. The usual procedure for the solution of such problems is to guess values for the two unknowns at the wall, to make a step-by-step integration of the equations and to correct the guessed values iteratively until the specified conditions are satisfied at "infinity". For boundary layers, an acceptable "infinity" is mercifully close to the

wall. Here, an adaptive approach for specifying infinity was used. Initially a value of $E_\infty = 16{\cdot}0$ was specified, and values of $F''(0)$ and $G'(0)$ found such that

$$|F'(\infty)| < \varepsilon_1, |G(\infty)| < \varepsilon_1 \qquad (10)$$

were satisfied. The values of $F''(\infty)$ and $G'(\infty)$ were then examined, and if they were not smaller than a second bound ε_2, the value of E_∞ was increased (by 1·0) and the integration repeated.

If the values of $F''(0)$ and $G'(0)$ were not close to their correct values, intermediate results became obviously incorrect. Gross corrections to the starting values were made until an integration to E_∞ could be obtained without catastrophe. Small changes were then made to the starting values, a second complete integration obtained, and iterpolation used to force equation (10) to be satisfied.

Probably as a result of the coupling of equa-equations (7) and (8), the response of $F'(\infty)$ and $G(\infty)$ to changes in $F''(0)$ and $G'(0)$ is somewhat unexpected. A typical situation is shown in Fig. 3, where, for a particular set of values of the parameters, the values at "infinity" of F', F'', G and G' are plotted against $F''(0)$ and $G'(0)$. It can be seen that $F'(\infty)$ is almost independent of $F''(0)$, but very sensitive to $G'(0)$. (This situation does not exist unless $F''(0)$ and $G'(0)$ are close to their correct values.) Thus, interpolation from two successive values of $F'(\infty)$ to improve the estimate of $F''(0)$ is not successful. However, it was found entirely satisfactory to adjust $G'(0)$ until $F'(\infty)$ satisfied equation (10), adjust $F''(0)$ until $G'(\infty)$ satisfied equation (10), and repeat both processes until the two conditions in equation (10) were satisfied simultaneously. At a later stage in the computations a different iteration scheme for controlling convergence was tried, using a technique somewhat similar to that described by Nachtsheim and Swigert [10]. The same convergence criteria were used with both iteration schemes. The results were virtually identical, of course, the latter iteration scheme giving a larger range of convergence.

The integration of equations (7) and (8) was

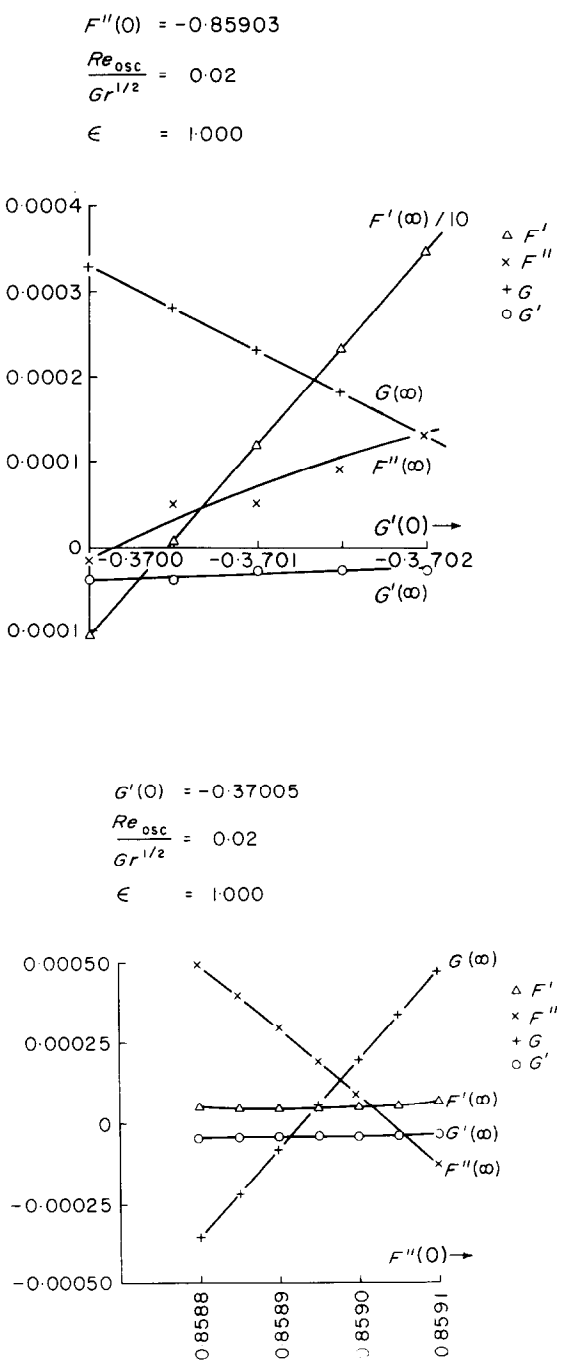

FIG. 3. Effect of initial values of $F''(0)$ and $G'(0)$ on values at "infinity" (a) and (b).

achieved by replacing them by a set of five first-order equations, and using a fourth-order Runge–Kutta computer-library subroutine. A step size in E of 0·001 up to $E = 0{\cdot}5$, and of 0·05 thereafter, was found sufficient in order to ensure convergence (in the sense that the solution becomes independent of further reductions in step size). This was particularly true with large values of λ, for which rapid fluctuations occur in $f(\lambda E)$ at small values of E. The convergence criteria adopted were $\varepsilon_1 = 0{\cdot}0001$ and $\varepsilon_2 = 0{\cdot}0005$.

4. RESULTS FOR THE FIRST-ORDER EQUATIONS

Solutions of equations (7)–(9) have been computed within the following ranges of variables, all for $Pr = 0{\cdot}7$ and for vertically and horizontally propagated sound fields:

$$5 \leqslant \lambda \leqslant 50$$
$$0 \leqslant K < 2000,$$

the maximum range examined of the streaming strength parameter K being so that the corresponding range of the streaming strength parameter ε is $0 \leqslant \varepsilon \leqslant 2{\cdot}5$. This range of variables was chosen primarily to correspond with some experimental data, but also to explore somewhat the effects of λ. In addition, some solutions were obtained for $Pr = 2{\cdot}85$, $\lambda = 6, 0 \leqslant \varepsilon \leqslant 5{\cdot}0$ which are of interest for a possible mass-transfer experiment.

There is a great effect of the Reynolds stresses on the flow pattern. These effects are illustrated in graphs of the velocity and temperature distributions, Figs. 4–9, for λ's in the vicinity of 20, together with corresponding graphs for undisturbed natural convection. The boundary layer really involves two characteristic thicknesses, one being characteristic of the Reynolds stress distribution (see Fig. 2) and the other of the natural convection. To display the effects in both layers in similar detail it has been convenient to use semi-logarithmic coordinates for the graphs. Regions of flow reversal can be identified easily ($F' < 0$). The temperature gradients, G', through the regions of greatly changed flow ($E < 0{\cdot}3$, say) are very nearly constant, showing that in this region conduction is far more significant than convection. Figures 10 and 11 also help to give some perspective on the results: both are for vertical oscillations. Figure 10 illustrates that changes in the temperature gradient at the

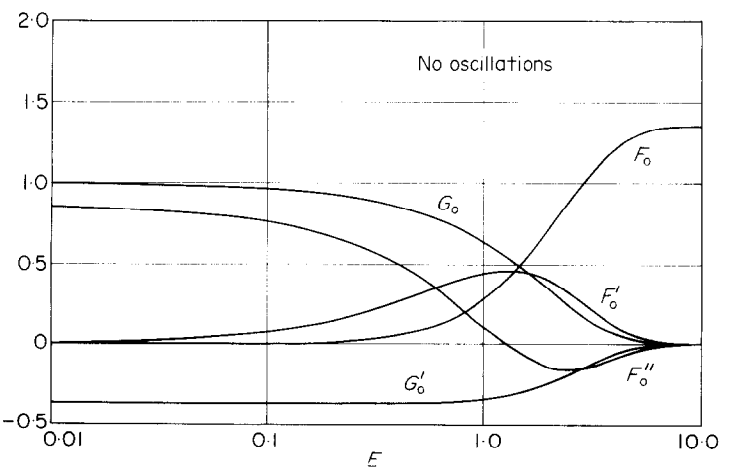

FIG. 4. Variables obtained in solution of the momentum and energy equations for steady natural convection in the absence of oscillations. The space variable has been plotted on a logarithmic scale to facilitate comparison with the corresponding solutions in the presence of oscillations.

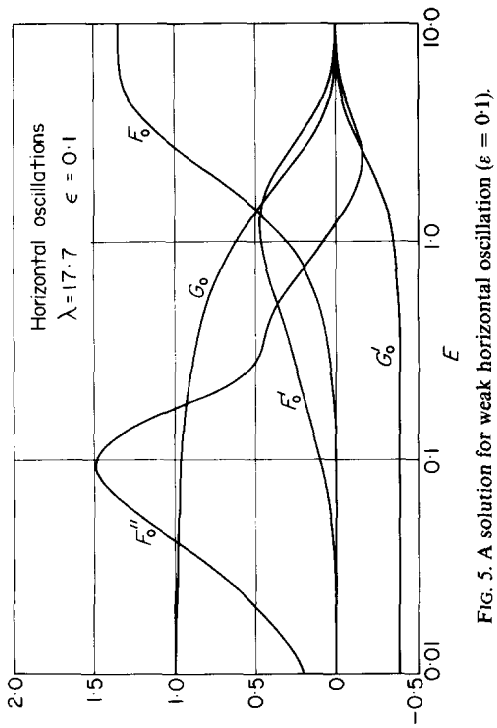

FIG. 5. A solution for weak horizontal oscillation ($\varepsilon = 0{\cdot}1$).

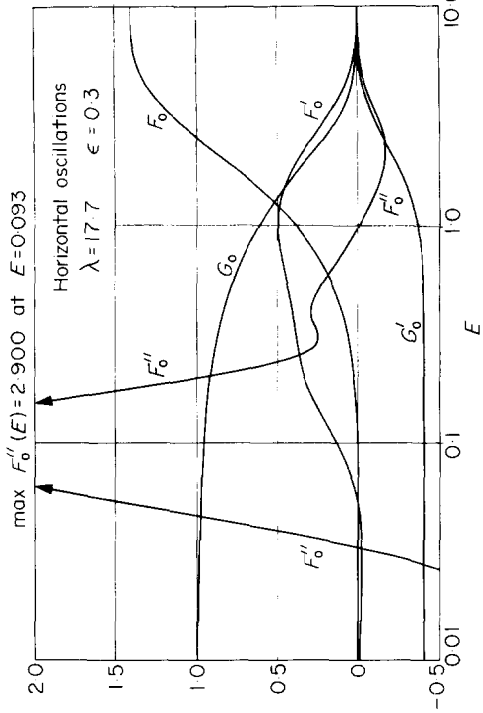

FIG. 6. As Fig. 5, but with ε increased to 0·3.

FIG. 7. As Figs. 5 and 6, but with ε increased to 1·0.

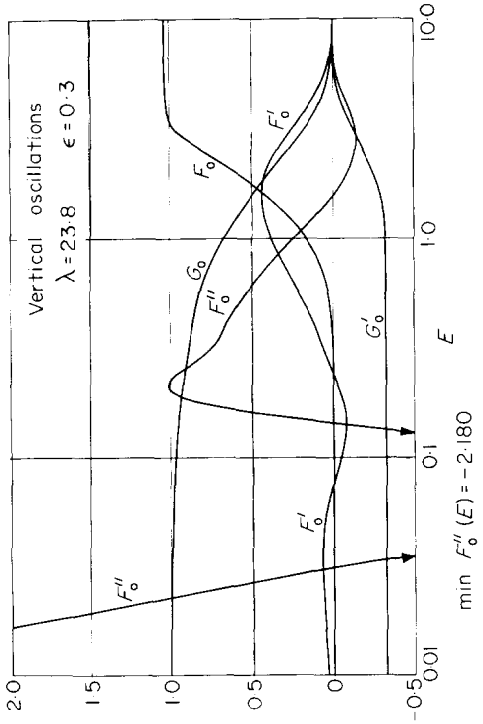

FIG. 8. A solution for mild vertical oscillations ($\varepsilon = 0{\cdot}3$).

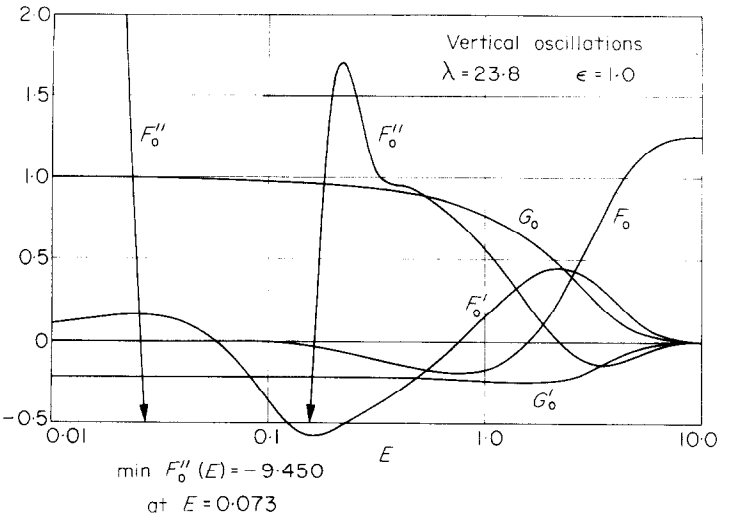

FIG. 9. As Fig. 8, but with ε increased to 1·0.

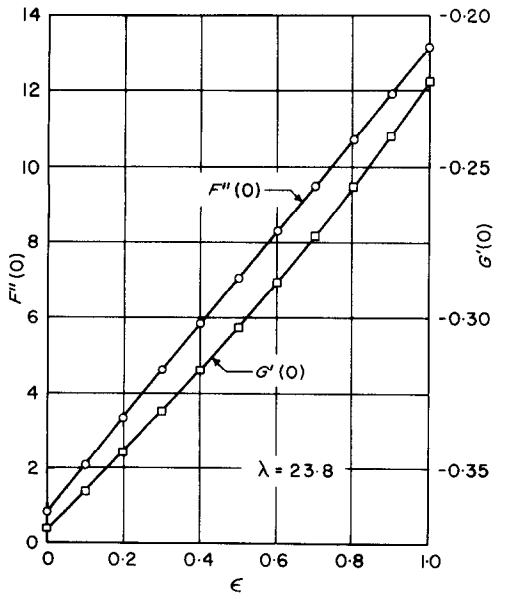

FIG. 10. Computed temperature gradient at the wall, $G'(0)$, and skin friction, $F''(0)$.

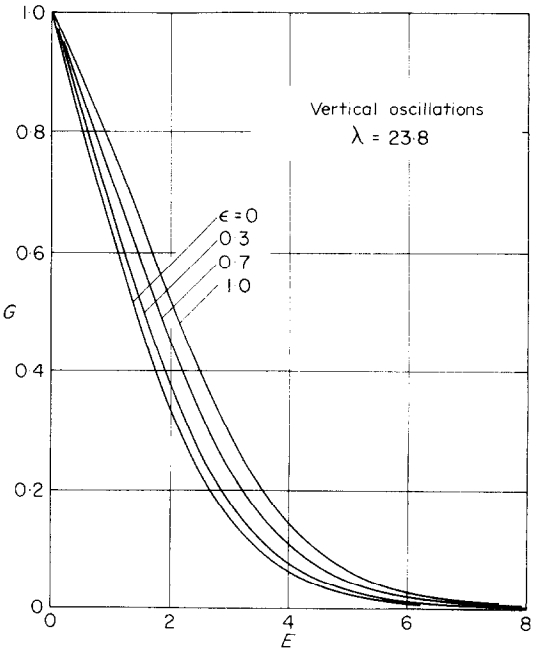

FIG. 11. Temperature profiles for various ε with vertical oscillations.

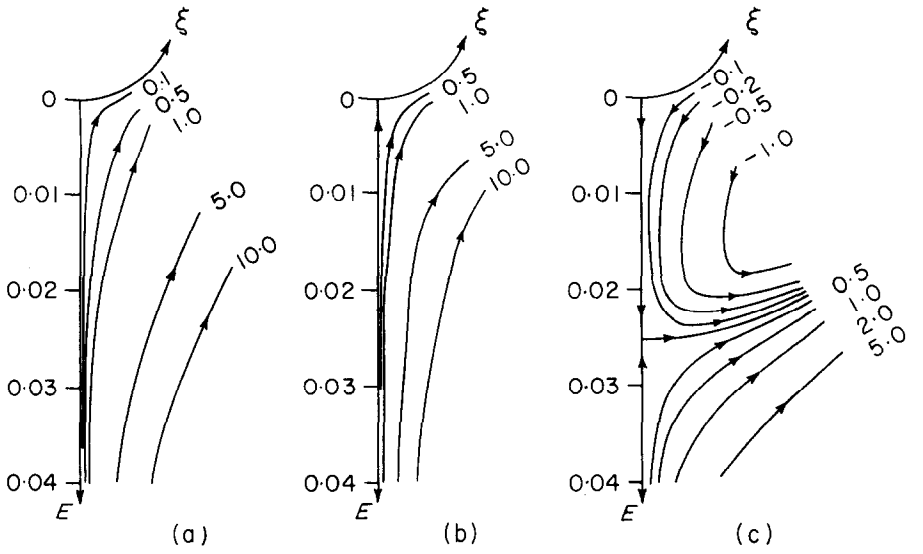

FIG. 12. (a) Natural convection, no sound. (b) Vertical sound field, $\lambda = 23{\cdot}8$, $\varepsilon = 4\ Re_s/Gr^{\frac{1}{4}} = 0{\cdot}14$. (c) Horizontal sound field, $\lambda = 30$, $\varepsilon = 0{\cdot}10$. The values of E in the range of these graphs is small and shows mainly what happens in the oscillating boundary-layer region. The numbers on the stream-lines are values of the stream function.

wall, $G'(0)$, and in the skin friction, $F''(0)$, are almost linear with ε when ε is small; however, over the range of ε shown, the heat-transfer rate decreases by about one-half while the friction increases by about 13 times. Figure 11 shows how the temperature profile changes; the profiles have smaller slopes near the origin as ε is increased, but the relative shift of the profiles seems to remain almost constant for $E > 1$.

The motion is most vividly displayed by charts of the streamline distribution. A chart of the streamlines which result from the imposed oscillations, in the absence of buoyancy, has been shown in Fig. 1. The streamline patterns

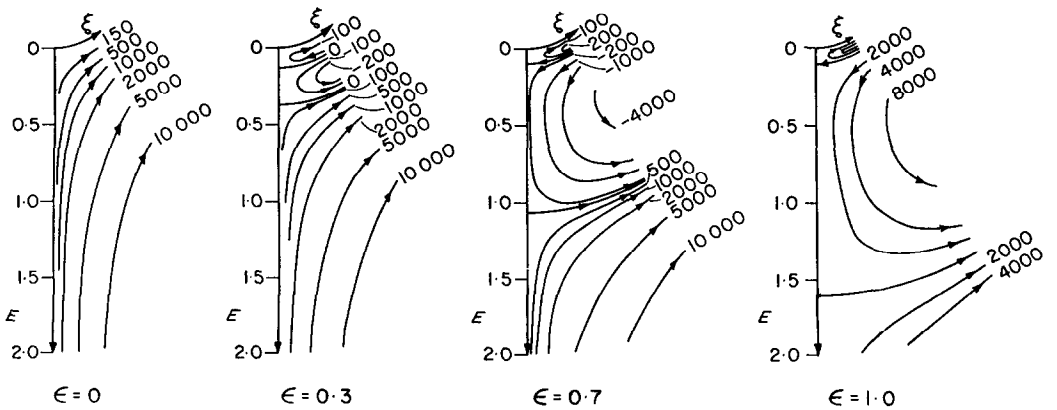

FIG. 13. Vertical sound field, $\lambda = 23{\cdot}8$. The streamline patterns illustrate the growth of a reversed flow bubble at the bottom of a heated cylinder as ε is increased from 0 to 1·0.

for the combined effects of buoyancy and Reynolds stresses can be computed from the solutions of equations (7)–(9), since

$$\frac{\psi}{Gr^{\frac{1}{4}}\nu} = \xi F(E).$$

Streamlines computed in this way for $F_0(E)$ are shown in Figs. 12 and 13. The solution $F(E)$ is asymptotically valid as $\xi \to 0$, and to emphasize this the streamlines have been shown only within 30° from the origin. The charts have been plotted in polar coordinates which give the boundary layer the appearance of extending over a large radius-ratio. This is convenient for examining streamline behaviour, but should not be used for literal interpretation as the physical plane: the boundary layer assumptions used require that the boundary layer be thin compared with the cylinder radius.

The principal features of the streamline patterns should be noted. For very weak sound fields the flow pattern is hardly changed at all. Once ε becomes sufficiently large, however, at least one region of reversed flow develops. (A region of reversed flow is one having closed streamlines, or which contains regions where the azimuthal component of velocity is negative.) For horizontal oscillations, this region of reversed flow is confined to a small range of E and corresponds to the inner streaming motion of the isothermal case. For vertical oscillations *two* regions of reversed flow are found. There is one small region close to the wall, similar to that found with horizontal oscillations but opposite in direction. The other region of reversed flow is more extensive, and grows rapidly with increase in ε. The outer acoustic streaming pattern associated with isothermal vertical oscillations involves a radial outflow at $\xi = 0$; if this outflow were hot, so that it had buoyancy which opposed its motion, it might be expected to stop its descent at some point and turn to move azimuthally round the cylinder. Thus the flow pattern found in the computer solution at larger ε corresponds *qualitatively* to what could be expected by superposition of buoyancy effects on the isothermal acoustic streaming pattern. The same comment can be applied to the results for horizontal oscillations. The presence of regions of reversed flow is found in the first-order solutions only when a sufficient value of ε is reached, this value depending upon λ and the direction of the applied oscillations. This suggests by itself that there may be critical conditions involved, i.e. that there is a critical ε for the onset of reversed flow. An examination of the flow field with higher-order equations taken into account indicates that the reversed flow develops first near the stagnation point and grows into the region $\xi > 0$ as ε increases.

The most dramatic changes in the flow pattern occur at values of E where the flow velocities are small, and pure conduction largely smothers changes in the convective pattern, so that the isotherms appear to be *relatively* insensitive to the flow changes. For the solutions of the first-order equations the isotherms are simply circular, and do not reveal interesting features when seen in a polar graph.

One is tempted to suggest that the flow patterns must tend to those of simple acoustic streaming as $\varepsilon \to \infty$, because this presents the situation where buoyancy effects become negligible. However, the ratio of the orders of magnitude of the inertia terms to the Reynolds stress terms is ε/λ^2, and it is only when this ratio is very small that the streaming motion can be expected to follow the pattern described by Stuart [4]. The requirement that $\varepsilon/\lambda^2 \ll 1$ corresponds in physical terms to the requirement that $a/d \ll 1$. If the computer solutions are examined as $\varepsilon \to \infty$ with λ held constant, the flow patterns cannot be expected to tend to those of Stuart. Some computations were made to assess quantitatively the effects of finite ε/λ^2 in the solution of the momentum equation with the buoyancy term (G) omitted. These showed that the magnitude of the wall shear stress increases beyond that associated with Stuart's asymptotic analysis, and that the flow at large E corresponds closely to the exponential decay in Stuart's solution when the origin of his ζ variable coincides with

that of E as used here. The maximum velocity, (F'/ε), in the outer streaming is slightly diminished; for $\varepsilon/\lambda^2 = 0{\cdot}001596$ the maximum velocity was about 0·696, and for ε/λ^2 twice as large ($\varepsilon = 1$, $\lambda = 17{\cdot}7$) it fell to about 0·664. A consequence of these changes in the velocity is that the separating streamline between the inner and outer streaming motions moves away somewhat from the cylinder surface compared with $\varepsilon/\lambda^2 \to 0$. However, at the appropriate limits the computed results are in accord with previous results.

All computed results are represented in the set of tables, Tables 1–13. These list all boundary

Table 1a. $\lambda = 50$, Pr = 0·7; *Horizontal sound field boundary values*

ε	$G'(0)$	$F''(0)$	$F(\infty)$
0·0	−0·37023	0·85935	1·3484
0·05	−0·37707	−0·42433	1·3537
0·10	−0·38382	−1·70910	1·3603
0·20	−0·39709	−4·28201	1·3744
0·30	−0·41006	−6·85926	1·3856
0·40	−0·42275	−9·44058	1·3961
0·50	−0·43517	−12·02581	1·4078
0·60	−0·44735	−14·61477	1·4213
0·70	−0·45929	−17·20734	1·4333
0·80	−0·47100	−19·80339	1·4453
0·90	−0·48250	−22·40288	1·4540
1·00	−0·49379	−25·00552	1·4671
1·20	−0·51580	−30·22008	1·4940
1·40	−0·53709	−35·44650	1·5194
1·60	−0·55772	−40·68411	1·5473
1·80	−0·57775	−45·93234	1·5730
2·00	−0·59719	−51·19048	1·6024
2·20	−0·61609	−56·45839	1·6297
2·40	−0·63449	−61·73547	1·6591

Table 1b. $\lambda = 50$; Pr = 0·7; $\varepsilon = 1{\cdot}0$; *Horizontal sound field*

E	F	F'	G	G'
0·0	0·0	0·0	1·00000	−0·49380
0·01	−0·00084	−0·12954	0·99506	−0·49380
0·02	−0·00192	−0·05826	0·99012	−0·49380
0·03	−0·00163	0·12854	0·98519	−0·49381
0·04	0·00076	0·34675	0·98025	−0·49381
0·05	0·00522	0·53749	0·97531	−0·49380
0·07	0·01848	0·75107	0·96543	−0·49372
0·10	0·04189	0·77757	0·95063	−0·49341
0·15	0·07947	0·73794	0·92598	−0·49236
0·20	0·11630	0·73502	0·90140	−0·49068
0·25	0·15290	0·72890	0·87692	−0·48837
0·35	0·22508	0·71419	0·82839	−0·48195
0·50	0·33024	0·68700	0·75707	−0·46808
1·00	0·64527	0·56781	0·54011	−0·39393
2·00	1·08261	0·31499	0·23890	−0·21199
4·00	1·40323	0·06119	0·03495	−0·03510
6·00	1·45860	0·00912	0·00457	−0·00468
8·00	1·46649	0·00122	0·00058	−0·00060
10·00	1·46749	0·00014	0·00007	−0·00008
12·00	1·46758	0·00001	0·00000	−0·00001

Table 1c. $\lambda = 50$; Pr = 0·7; $\varepsilon = 2{\cdot}4$; *Horizontal sound field*

E	F	F'	G	G'
0·0	0·0	0·0	1·00000	−0·63449
0·01	−0·00211	−0·32805	0·99366	−0·63450
0·02	−0·00495	−0·17397	0·98731	−0·63451
0·03	−0·00467	0·25748	0·98096	−0·63454
0·04	0·00045	0·76449	0·97462	−0·63455
0·05	0·01040	1·20574	0·96827	−0·63452
0·07	0·04023	1·68587	0·95559	−0·63431
0·10	0·09220	1·70283	0·93657	−0·63343
0·15	0·17240	1·53592	0·90496	−0·63048
0·20	0·24737	1·46383	0·87355	−0·62586
0·25	0·31872	1·39019	0·84240	−0·61969
0·35	0·45081	1·25416	0·78122	−0·60317
0·50	0·62518	1·07547	0·69312	−0·56991
1·00	1·04639	0·64588	0·44376	−0·42272
2·00	1·44984	0·22939	0·15818	−0·17228
4·00	1·63807	0·02559	0·01632	−0·01897
6·00	1·65788	0·00232	0·00150	−0·00188
8·00	1·65934	0·00003	0·00004	−0·00018
10·00	1·65919	−0·00007	−0·00010	−0·00002
12·00	1·65914	0·00005	−0·00012	−0·00000

Table 2a. $\lambda = 25{\cdot}0$; Pr = 0·70; *Horizontal sound field boundary values*

ε	$G'(0)$	$F''(0)$	$F(\infty)$
0·0	−0·37023	0·85935	1·3484
0·05	−0·37648	0·20070	1·3532
0·10	−0·38266	−0·45891	1·3595
0·20	−0·39476	−1·78099	1·3718
0·30	−0·40657	−3·10672	1·3834
0·40	−0·41809	−4·43592	1·3942
0·50	−0·42934	−5·76847	1·4016
0·60	−0·44034	−7·10401	1·4181
0·70	−0·45111	−8·44265	1·4297
0·80	−0·46165	−9·78421	1·4416
0·90	−0·47198	−11·12856	1·4531
1·00	−0·48209	−12·47558	1·4654
1·10	−0·49201	−13·82524	1·4743
1·20	−0·50175	−15·17730	1·4897
1·40	−0·52071	−17·88882	1·5106
1·60	−0·53898	−20·60936	1·5351
1·80	−0·55668	−23·33855	1·5597
2·00	−0·57380	−26·07590	1·5834
2·50	−0·61433	−32·95189	1·6586

Table 2b. $\lambda = 25{\cdot}0$; Pr = 0·70; $\varepsilon = 1{\cdot}0$; *Horizontal sound field*

E	F	F'	G	G'
0·0	0·0	0·0	1·00000	−0·48209
0·01	−0·00052	−0·09386	0·99518	−0·48209
0·02	−0·00168	−0·12903	0·99036	−0·48209
0·04	−0·00382	−0·05756	0·98072	−0·48211
0·07	−0·00138	0·23854	0·96625	−0·48215
0·10	0·01047	0·53698	0·95179	−0·48211
0·15	0·04454	0·76890	0·92769	−0·48166
0·25	0·12116	0·73777	0·87964	−0·47886
0·50	0·29950	0·69233	0·76181	−0·46149
1·0	0·61786	0·57554	0·54682	−0·39237
2·0	1·06346	0·32292	0·24444	−0·21462
5·0	1·43723	0·02584	0·01337	−0·01340
8·0	1·46343	0·00172	0·00079	−0·00063
12·0	1·46539	−0·00003	0·00018	−0·00001

Table 2c. $\lambda = 25{\cdot}0$; Pr = 0·70; $\varepsilon = 2{\cdot}5$; *Horizontal sound field*

E	F	F'	G	G'
0·0	0·0	0·0	1·00000	−0·61433
0·01	−0·00139	−0·25219	0·99386	−0·61433
0·02	−0·00455	−0·35753	0·98771	−0·61434
0·04	−0·01093	−0·21319	0·97543	−0·61441
0·07	−0·00768	0·47679	0·95699	−0·61456
0·10	0·01762	1·17416	0·93855	−0·61451
0·15	0·09244	1·67691	0·90785	−0·61338
0·25	0·25254	1·46540	0·84683	−0·60592
0·5	0·57220	1·12217	0·70009	−0·56307
1·0	1·01142	0·67326	0·45181	−0·42401
2·0	1·43242	0·24007	0·16294	−0·17584
5·0	1·64843	0·00955	0·00555	−0·00623
8·0	1·65755	0·00068	0·00033	−0·00019
12·0	1·65856	0·00001	0·00016	−0·00000

Table 3a. $\lambda = 25{\cdot}00$; Pr = 0·70; *Vertical sound field boundary values*

ε	$G'(0)$	$F''(0)$	$F(\infty)$
0·0	−0·37023	0·85935	1·3484
0·05	−0·36389	1·51699	1·3435
0·1	−0·35746	2·17356	1·3376
0·2	−0·34433	3·48350	1·3290
0·3	−0·33079	4·78881	1·3178
0·4	−0·31681	6·08921	1·3081
0·5	−0·30237	7·38431	1·3010
0·6	−0·28741	8·67359	1·2893

Table 3b. $\lambda = 25{\cdot}0$; Pr = 0·70; $\varepsilon = 0{\cdot}5$; *Vertical sound field*

E	F	F'	G	G'
0·0	0·0	0·0	1·00000	−0·30237
0·02	0·00107	0·08715	0·99395	−0·30237
0·04	0·00281	0·07345	0·98791	−0·30236
0·06	0·00362	0·00158	0·98186	−0·30235
0·08	0·00277	−0·08643	0·97581	−0·30233
0·10	0·00025	−0·16113	0·96976	−0·30233
0·15	−0·01019	−0·22847	0·95465	−0·30237
0·20	−0·02071	−0·18376	0·93952	−0·30254
0·25	−0·02836	−0·12377	0·92439	−0·30280
0·30	−0·03330	−0·07585	0·90924	−0·30313
0·35	−0·03605	−0·03462	0·89408	−0·30350
0·40	−0·03680	0·00453	0·87889	−0·30389
0·50	−0·03263	0·07757	0·84847	−0·30464
0·70	−0·00440	0·19946	0·78743	−0·30552
1·00	0·07618	0·32751	0·69596	−0·30343
2·00	0·48424	0·42317	0·41297	−0·25068
5·00	1·20123	0·08176	0·04024	−0·03521
8·00	1·29412	0·00673	0·00272	−0·00247
12·00	1·30096	0·00000	0·00008	−0·00006

Table 4a. $\lambda = 23{\cdot}8$; Pr = 0·7; *Vertical sound field boundary values*

ε	$G'(0)$	$F''(0)$	$F(\infty)$
0·0	−0·37021	0·85932	1·3415
0·14	−0·35246	2·61417	1·3517
0·18	−0·34723	3·11399	1·3447
0·20	−0·34455	3·36352	1·3250
0·225	−0·34124	3·67535	1·3256
0·250	−0·33788	3·98681	1·3163
0·275	−0·33451	4·29800	1·3127
0·300	−0·33117	4·60911	1·3339
0·400	−0·31725	5·84956	1·2980
0·500	−0·30296	7·08499	1·3057
0·600	−0·28809	8·31466	1·2899
0·700	−0·27264	9·53804	1·2696
0·800	−0·25658	10·75460	1·2663
0·900	−0·23980	11·96348	1·2800
1·0	−0·22213	13·16345	1·2656

values determined, together with a very small sampling of velocity and temperature profiles.

5. COMPARISON WITH EXPERIMENTS

The most important characteristic of these computations is that they are closely similar to the results found in related experiments [11–13]. Thus, in both theory and experiment, horizontal oscillations increase heat transfer at the bottom of the cylinder and vertical oscillations decrease

Table 4b. $\lambda = 23{\cdot}8$; Pr = 0·7; $\varepsilon = 0{\cdot}5$; *Vertical sound field*

E	F	F'	G	G'
0·0	0·0	0·0	1·00000	−0·30296
0·02	0·00105	0·08664	0·99394	−0·30296
0·04	0·00284	0·08014	0·98788	−0·30295
0·06	0·00387	0·01694	0·98182	−0·30294
0·08	0·00339	−0·06577	0·97576	−0·30292
0·10	0·00130	−0·14035	0·96971	−0·30291
0·15	−0·00840	−0·22126	0·95456	−0·30294
0·20	−0·01886	−0·18634	0·93941	−0·30309
0·25	−0·02666	−0·12678	0·92425	−0·30333
0·30	−0·03166	−0·07606	0·90907	−0·30364
0·35	−0·03440	−0·03421	0·89388	−0·30400
0·40	−0·03513	0·00476	0·87867	−0·30437
0·50	−0·03095	0·07764	0·84820	−0·30509
0·70	−0·00271	0·19950	0·78708	−0·30589
1·00	0·07786	0·32744	0·69551	−0·30369
2·00	0·48568	0·42278	0·41244	−0·25062
5·00	1·20191	0·08180	0·04011	−0·03513
8·00	1·29558	0·00712	0·00279	−0·00246
12·00	1·30424	0·00050	0·00006	−0·00006
16·00	1·30599	0·00034	−0·00001	−0·00000

Table 4c. $\lambda = 23{\cdot}8$; Pr = 0·7; $\varepsilon = 1{\cdot}0$; *Vertical sound field*

E	F	F'	G	G'
0·0	0·0	0·0	1·00000	−0·22213
0·02	0·00189	0·15335	0·99556	−0·22213
0·04	0·00489	0·12082	0·99111	−0·22212
0·06	0·00597	−0·02472	0·98667	−0·22210
0·08	0·00365	−0·20887	0·98223	−0·22208
0·10	−0·00227	−0·37636	0·97779	−0·22208
0·15	−0·02757	−0·58213	0·96668	−0·22219
0·20	−0·05650	−0·55337	0·95557	−0·22252
0·25	−0·08210	−0·47109	0·94443	−0·22306
0·30	−0·10394	−0·40613	0·93326	−0·22379
0·35	−0·12294	−0·35488	0·92204	−0·22468
0·40	−0·13947	−0·30676	0·91079	−0·22572
0·50	−0·16542	−0·21307	0·88810	−0·22815
0·70	−0·19084	−0·04577	0·84190	−0·23400
1·00	−0·17316	0·15349	0·77028	−0·24337
2·00	0·16558	0·44013	0·51953	−0·24805
5·00	1·09248	0·13107	0·06651	−0·05476
8·00	1·29091	0·01286	0·00499	−0·00441
12·00	1·26535	0·00036	0·00013	−0·00013
16·00	1·26564	0·00000	−0·00001	−0·00000

the local heat transfer. Corresponding changes of thermal boundary layer thickness are predicted and observed. In addition, observations have been made for vertical oscillations which suggested the presence of a "bubble" of reversed

Table 5a. $\lambda = 20$; Pr = 0·7; *Horizontal sound field boundary values*

ε	$G'(0)$	$F''(0)$	$F(\infty)$
0·0	−0·37023	0·85925	1·3421
0·05	−0·37619	0·32583	1·3497
0·10	−0·38209	−0·20853	1·3568
0·20	−0·39363	−1·27992	1·3683
0·30	−0·40487	−2·35471	1·3771
0·40	−0·41583	−3·43256	1·3919
0·50	−0·42653	−4·51357	1·4003
0·60	−0·43697	−5·59742	1·4113
0·70	−0·44718	−6·68394	1·4274
0·80	−0·45716	−7·77321	1·4379
0·90	−0·46693	−8·86510	1·4455
1·00	−0·47650	−9·95925	1·4628

Table 5b. $\lambda = 20$; Pr = 0·7; $\varepsilon = 1{\cdot}0$; *Horizontal sound field*

E	F	F'	G	G'
0·0	0·0	0·0	1·00000	−0·47650
0·02	−0·00147	−0·12122	0·99047	−0·47650
0·04	−0·00392	−0·10453	0·98094	−0·47652
0·06	−0·00500	0·00902	0·97141	−0·47655
0·08	−0·00323	0·17311	0·96188	−0·47658
0·10	0·00199	0·34733	0·95235	−0·47659
0·15	0·02837	0·67111	0·92852	−0·47636
0·20	0·06535	0·77789	0·90472	−0·47558
0·25	0·10422	0·76737	0·88097	−0·47417
0·30	0·14181	0·73730	0·85731	−0·47213
0·35	0·17817	0·71946	0·83377	−0·46950
0·40	0·21390	0·71064	0·81037	−0·46628
0·50	0·28423	0·69505	0·76413	−0·45822
0·70	0·41917	0·65303	0·67457	−0·43616
1·00	0·60426	0·57936	0·55012	−0·39157
2·00	1·05389	0·32675	0·24719	−0·21593
5·00	1·43362	0·02647	0·01364	−0·01364
8·00	1·46059	0·00181	0·00081	−0·00065
12·00	1·46274	0·00001	0·00019	−0·00001

Table 6a. $\lambda = 20$; Pr = 0·7; *Vertical sound field boundary values*

ε	$G'(0)$	$F''(0)$	$F(\infty)$
0·0	−0·37023	0·85935	1·3484
0·1	−0·35803	1·92345	1·3372
0·2	−0·34546	2·98360	1·3287
0·3	−0·33249	4·03948	1·3183
0·4	−0·31908	5·09085	1·3126
0·5	−0·30521	6·13721	1·3033
0·6	−0·29081	7·17818	1·2915
0·7	−0·27584	8·21333	1·2876
0·8	−0·26022	9·24187	1·2764
0·9	−0·24386	10·26313	1·2687
1·0	−0·22666	11·27608	1·2636

Table 6b. $\lambda = 20$; Pr = 0·7; $\varepsilon = 1{\cdot}0$; *Vertical sound field*

E	F	F'	G	G'
0·0	0·0	0·0	1·00000	−0·22666
0·02	0·00173	0·14716	0·99547	−0·22666
0·04	0·00496	0·15563	0·99093	−0·22665
0·06	0·00730	0·06646	0·98640	−0·22663
0·08	0·00727	−0·07399	0·98187	−0·22661
0·10	0·00427	−0·22529	0·97734	−0·22659
0·15	−0·01463	−0·49472	0·96601	−0·22662
0·20	−0·04151	−0·55055	0·95467	−0·22684
0·25	−0·06779	−0·49156	0·94332	−0·22728
0·30	−0·09042	−0·41512	0·93194	−0·22791
0·35	−0·10956	−0·35309	0·92052	−0·22871
0·40	−0·12592	−0·30247	0·90907	−0·22966
0·50	−0·15152	−0·21047	0·88599	−0·23191
0·70	−0·17644	−0·04332	0·83908	−0·23739
1·00	−0·15813	0·15519	0·76653	−0·24613
2·00	0·18025	0·43771	0·51430	−0·24821
5·00	1·09608	0·12855	0·06517	−0·05378
8·00	1·25063	0·01227	0·00485	−0·00432
12·00	1·26358	0·00010	0·00009	−0·00013
13·00	1·26356	−0·00009	0·00000	−0·00005

Table 7. $\lambda = 18{\cdot}0$; Pr = 0·7; *Horizontal sound field*

ε	$G'(0)$	$F'(0)$	$F(\infty)$
1·0	−0·47346	−8·95042	1·4556

Table 8a. $\lambda = 17{\cdot}7$; Pr = 0·70; *Horizontal sound field boundary values*

ε	$G'(0)$	$F''(0)$	$F(\infty)$
0·0	−0·37023	0·85925	1·3415
0·05	−0·37603	0·38347	1·3519
0·1	−0·38172	−0·09320	1·3577
0·2	−0·39291	−1·04912	1·3691
0·3	−0·40379	−2·00815	1·3826
0·4	−0·41440	−2·97025	1·3932
0·5	−0·42474	−3·93520	1·4047
0·6	−0·43483	−4·90292	1·4142
0·7	−0·44469	−5·87323	1·4263
0·8	−0·45432	−6·84614	1·4327
0·9	−0·46374	−7·82136	1·4441
1·0	−0·47296	−8·79890	1·4563
1·1	−0·48199	−9·77865	1·4677
1·2	−0·49084	−10·76063	1·4769
1·3	−0·49951	−11·74465	1·4888
1·4	−0·50801	−12·73065	1·5009
1·5	−0·51634	−13·71858	1·5149
1·6	−0·52453	−14·70840	1·5271
1·7	−0·53256	−15·70009	1·5393
1·8	−0·54045	−16·69354	1·5513
1·9	−0·54821	−17·68874	1·5632
2·0	−0·55583	−18·68558	1·5757
2·1	−0·56334	−19·68420	1·5838
2·2	−0·57071	−20·68434	1·5962
2·3	−0·57796	−21·68599	1·6096
2·4	−0·58507	−22·68907	1·6235
2·5	−0·59209	−23·69370	1·6376

flow underneath the cylinder when the intensity was large enough [13], corresponding to the reversed flow region computed here.

However, it should be noted that at the highest intensities achieved in the experiments with vertical sound fields an oscillatory, unstable motion was observed to develop in the bottom stagnation region [13]. The framework used for the analysis presented here precludes calculation of instability of the secondary motion, and one should not expect the close similarity between analysis and experiment to persist to indefinitely large values of ε (supposing that solutions were computed that far). The experimental observations suggest that the next stage in development of analysis should be to examine the stability of the flow, as instability apparently can develop at values of ε below those at which (with vertical oscillations) the downflow jet would break out of the boundary layer region and vitiate the

Table 8b. $\lambda = 17{\cdot}7$; Pr = 0·70; $\varepsilon = 1{\cdot}0$; *Horizontal sound field*

E	F	F'	G	G'
0·0	0·0	0·0	1·00000	−0·47296
0·02	−0·00135	−0·11466	0·99054	−0·47297
0·04	−0·00384	−0·11820	0·98108	−0·47298
0·06	−0·00551	−0·03765	0·97162	−0·47302
0·08	−0·00500	0·09470	0·96216	−0·47305
0·10	−0·00159	0·24835	0·95270	−0·47308
0·15	0·01982	0·58501	0·92905	−0·47295
0·20	0·05394	0·75039	0·90541	−0·47235
0·25	0·09255	0·77863	0·88182	−0·47114
0·30	0·13095	0·75442	0·85831	−0·46930
0·35	0·16798	0·72837	0·83490	−0·46685
0·40	0·20397	0·71281	0·81163	−0·46382
0·50	0·27436	0·69584	0·76562	−0·45611
0·70	0·40967	0·65513	0·67641	−0·43475
1·00	0·59543	0·58173	0·55225	−0·39105
2·00	1·04747	0·32893	0·24894	−0·21679
5·00	1·42943	0·02618	0·01369	−0·01383
8·00	1·45500	0·00136	0·00064	−0·00066
12·00	1·45625	0·00002	−0·00000	−0·00001

Table 8c. $\lambda = 17{\cdot}7$; Pr = 0·70; $\varepsilon = 2{\cdot}5$; *Horizontal sound field*

E	F	F'	G	G'
0·0	0·0	0·0	1·00000	−0·59209
0·02	−0·00371	−0·32029	0·98816	−0·59210
0·04	−0·01095	−0·36213	0·97632	−0·59216
0·06	−0·01678	−0·19314	0·96447	−0·59228
0·08	−0·01781	0·10600	0·95262	−0·59243
0·10	−0·01219	0·45906	0·94077	−0·59256
0·15	0·03134	1·22608	0·91115	−0·59243
0·20	0·10306	1·56980	0·88155	−0·59106
0·25	0·18266	1·57658	0·85207	−0·58812
0·30	0·25870	1·45863	0·82277	−0·58358
0·35	0·32860	1·34231	0·79373	−0·57760
0·40	0·39348	1·25785	0·76503	−0·57034
0·50	0·51307	1·13906	0·70885	−0·55249
0·70	0·71995	0·93472	0·60276	−0·50656
1·00	0·96229	0·69300	0·46295	−0·42401
2·00	1·39954	0·25228	0·17027	−0·18087
5·00	1·62864	0·00994	0·00591	−0·00673
8·00	1·63727	0·00038	0·00020	−0·00022
12·00	1·63763	0·00002	0·00002	−0·00000

Table 9. $\lambda = 17{\cdot}7$; Pr = 0·70; *Vertical sound field boundary values*

ε	$G'(0)$	$F''(0)$	$F(\infty)$
0·0	−0·37023	0·85925	1·3415
0·05	−0·36435	1·33429	1·3417
0·1	−0·35839	1·80834	1·3381
0·2	−0·34619	2·75360	1·3315

Table 10. $\lambda = 10{\cdot}0$; Pr = 0·7; *Horizontal sound field boundary values*

ε	$G'(0)$	$F''(0)$	$F(\infty)$
0·010	−0·37114	0·80282	1·3324
0·015	−0·37160	0·77460	1·3304
0·020	−0·37204	0·74641	1·3265
0·025	−0·37252	0·71827	1·3325
0·030	−0·37299	0·69008	1·3368
0·035	−0·37345	0·66185	1·3362
0·040	−0·37391	0·63362	1·3359

N.B. Convergence criterion 0·0005.

boundary layer assumptions used in the analysis.

The comparison between this analysis and the available experiments cannot be carried further to the quantitative level, because there are some significant differences in some of the parameters. The Grashof numbers in the experiments were

Table 11a. $\lambda = 5{\cdot}0$; Pr = 0·7; *Horizontal sound field boundary values*

ε	$G'(0)$	$F''(0)$	$F(\infty)$
0·0	−0·37023	0·85935	1·3484
0·05	−0·37273	0·70669	1·3501
0·10	−0·37518	0·55379	1·3567
0·20	−0·37990	0·24703	1·3663
0·30	−0·38441	−0·06093	1·3742
0·40	−0·38873	−0·37001	1·3827
0·50	−0·39286	−0·68029	1·3851
0·60	−0·39682	−0·99146	1·3978
0·70	−0·40061	−1·30377	1·4044
0·80	−0·40424	−1·61713	1·4070
0·90	−0·40772	−1·93130	1·4203
1·00	−0·41105	−2·24652	1·4270

Table 11b. $\lambda = 5{\cdot}0$; Pr = 0·7; $\varepsilon = 1{\cdot}0$; *Horizontal sound field*

E	F	F'	G	G'
0·0	0·0	0·0	1·00000	−0·41105
0·02	−0·00042	−0·04014	0·99178	−0·41105
0·04	−0·00154	−0·07078	0·98356	−0·41106
0·08	−0·00517	−0·10471	0·96711	−0·41110
0·12	−0·00947	−0·10526	0·95067	−0·41118
0·16	−0·01321	−0·07726	0·93422	−0·41131
0·20	−0·01535	−0·02635	0·91776	−0·41148
0·25	−0·01458	0·06054	0·89718	−0·41170
0·30	−0·00904	0·16284	0·87659	−0·41187
0·40	0·01796	0·37524	0·83450	−0·41180
0·50	0·06482	0·55297	0·79427	−0·41065
0·70	0·19670	0·72496	0·71275	−0·40336
1·00	0·41140	0·67342	0·59509	−0·37829
2·0	0·92376	0·38138	0·28611	−0·23318
4·0	1·33185	0·08407	0·04672	−0·04489
8·0	1·42428	0·00239	0·00105	−0·00089
12·0	1·42698	0·00000	0·00018	−0·00002

Table 12a. $\lambda = 6{\cdot}0$; Pr = 2·85; *Horizontal sound field boundary values*

ε	$G'(0)$	$F''(0)$	$F(\infty)$
0·0	−0·60047	0·68998	0·7937
0·01	−0·60218	0·65407	0·7952
0·1	−0·61714	0·33041	0·8089
0·3	−0·64766	−0·39201	0·8416
0·5	−0·67467	−1·11868	0·8768
1·0	−0·72902	−2·95341	0·9671
1·5	−0·76841	−4·81263	1·0533
2·0	−0·79674	−6·69460	1·1336
2·5	−0·81671	−8·59773	1·2048
3·0	−0·83024	−10·52043	1·2746
3·5	−0·83866	−12·46177	1·3359
4·0	−0·84303	−14·42074	1·3915
4·5	−0·84395	−16·39656	1·4440
5·0	−0·84202	−18·38878	1·4912

Table 12b. $\lambda = 6{\cdot}0$; Pr = 2·85; $\varepsilon = 0{\cdot}0$

E	F	F'	G	G'
0·0	0·0	0·0	1·00000	−0·60047
0·02	0·00014	0·01360	0·98799	−0·60047
0·05	0·00084	0·03326	0·96998	−0·60045
0·10	0·00329	0·06410	0·93996	−0·60028
0·20	0·01251	0·11882	0·87998	−0·59901
0·40	0·04521	0·20279	0·76092	−0·58971
0·60	0·09166	0·25735	0·64497	−0·56744
1·0	0·20561	0·29988	0·43373	−0·47976
2·0	0·47759	0·22179	0·10927	−0·17765
3·0	0·64326	0·11602	0·01796	−0·03507
5·0	0·76294	0·02488	0·00027	−0·00059
8·0	0·79127	0·00223	−0·00000	−0·00000
12·0	0·79372	0·00001	−0·00000	−0·00000

Table 12c. $\lambda = 6{\cdot}0$; Pr = 2·85; $\varepsilon = 1{\cdot}0$; *Horizontal sound field*

E	F	F'	G	G'
0·0	0·0	0·0	1·00000	−0·72902
0·02	−0·00054	−0·05208	0·98542	−0·72902
0·05	−0·00297	−0·10450	0·96355	−0·72912
0·10	−0·00911	−0·12882	0·92708	−0·72974
0·20	−0·01714	−0·00114	0·85397	−0·73270
0·40	0·02911	0·45355	0·70703	−0·73346
0·60	0·14502	0·64872	0·56299	−0·69923
1·0	0·38255	0·50392	0·31661	−0·51443
2·0	0·72916	0·22254	0·04353	−0·09886
3·0	0·87495	0·08809	0·00379	−0·00974
5·0	0·95338	0·01290	0·00001	−0·00005
8·0	0·96610	0·00077	−0·00000	−0·00000
12·0	0·96709	0·00009	−0·00000	−0·00000

Table 12d. $\lambda = 6{\cdot}0$; Pr = 2·85; $\varepsilon = 2{\cdot}5$; *Horizontal sound field*

E	F	F'	G	G'
0·0	0·0	0·0	1·00000	−0·81671
0·02	−0·00042	−0·15419	0·98367	−0·81674
0·05	−0·00891	−0·32011	0·95916	−0·81708
0·10	−0·02859	−0·43598	0·91826	−0·81921
0·20	−0·06513	−0·21548	0·83584	−0·83067
0·40	−0·00823	0·76876	0·66668	−0·85645
0·60	0·19783	1·15854	0·49797	−0·81437
1·0	0·58959	0·73999	0·22767	−0·51081
2·0	1·01832	0·22702	0·01505	−0·04604
3·0	1·15055	0·06819	0·00057	−0·00202
5·0	1·20156	0·00579	−0·00004	−0·00000
8·0	1·20555	−0·00010	−0·00004	−0·00000
12·0	1·20483	−0·00014	−0·00004	−0·00000

Table 12e. $\lambda = 6{\cdot}0$; Pr = 2·85; $\varepsilon = 5{\cdot}0$; *Horizontal sound field*

E	F	F'	G	G'
0·0	0·0	0·0	1·00000	−0·84202
0·02	−0·00344	−0·33205	0·98316	−0·84208
0·05	−0·01929	−0·69861	0·95789	−0·84283
0·10	−0·06298	−0·98589	0·91565	−0·84764
0·20	−0·15258	−0·64483	0·82972	−0·87482
0·40	−0·09750	1·17556	0·64623	−0·95642
0·60	0·23273	1·86971	0·45495	−0·92627
1·0	0·82851	1·01850	0·16525	−0·48814
2·0	1·33939	0·22470	0·00475	−0·01870
3·0	1·45622	0·05074	0·00008	−0·00033
5·0	1·48869	0·00270	−0·00000	−0·00000
8·0	1·49075	0·00016	−0·00000	−0·00000
12·0	1·49124	0·00013	−0·00000	−0·00000

Table 13a. *Solution of* $F''' - F'^2 + FF'' - Kf(\lambda E) = 0$; $\lambda = 17{\cdot}7$; $\varepsilon = 0{\cdot}5$

E	F	F'	F''
0·0	0·0	0·0	−4·63050
0·01	−0·00021	−0·03851	−3·07906
0·02	−0·00072	−0·06185	−1·60808
0·04	−0·00210	−0·06794	0·88209
0·06	−0·00316	−0·03180	2·59492
0·08	−0·00320	0·03044	3·49966
0·10	−0·00187	0·10351	3·70521
0·17	0·01328	0·30392	1·65953
0·24	0·03681	0·34743	−0·12282
0·35	0·07302	0·30875	−0·31327
0·50	0·11683	0·27927	−0·15332
1·00	0·23794	0·20821	−0·12300
2·00	0·39516	0·11531	−0·06816
5·00	0·55700	0·01948	−0·01161
10·00	0·58758	0·00082	−0·00061
12·00	0·58836	0·00010	−0·00019

Entries of (F'/ε) here and in part c of this Table can be compared; they are both for the same value of ε/λ^2, but for different λ. The comparisons should be made at values of E which correspond to the same η.

finite, so that the natural convection results were not sufficiently close to the asymptotic, boundary-layer solution for differences to be ignored; and the streaming Reynolds numbers were small, rather than large. It is possible to extend the analysis to account for these differences, as is discussed below.

It is interesting to note that the velocities in the flow reversal region close to the cylinder surface are sufficiently small for conduction to

Table 13b. *Solution of* $F''' - F'^2 + FF'' - Kf(\lambda E) = 0$; $\lambda = 17{\cdot}7$; $\varepsilon = 1{\cdot}0$

E	F	F'	F''
0·0	0·0	0·0	−9·40725
0·01	−0·00042	−0·07849	−6·30437
0·02	−0·00147	−0·12663	−3·36237
0·04	−0·00432	−0·14173	1·61816
0·06	−0·00657	−0·07236	5·04419
0·08	−0·00687	0·04920	6·85411
0·10	−0·00446	0·19245	7·26580
0·17	0·02446	0·58328	3·17944
0·24	0·06946	0·66092	−0·37314
0·35	0·13742	0·57085	−0·73066
0·50	0·21698	0·49814	−0·38696
1·00	0·42154	0·33069	−0·27226
2·00	0·64688	0·14517	−0·11952
5·00	0·80825	0·01226	−0·01012
10·00	0·82278	0·00017	−0·00017
12·00	0·82282	0·00001	−0·00003

Table 13c. *Solution of* $F''' - F'^2 + FF'' - Kf(\lambda E) = 0$; $\lambda = 25$; $\varepsilon = 0{\cdot}9975$

E	F	F'	F''
0·0	0·0	0·0	−13·04763
0·01	−0·00055	−0·09960	−6·92839
0·02	−0·00180	−0·14057	−1·39951
0·04	−0·00428	−0·08075	6·63493
0·06	−0·00426	0·09438	10·15997
0·08	−0·00030	0·30095	10·00324
0·10	0·00759	0·48023	7·70039
0·17	0·05205	0·69310	−0·35005
0·24	0·09830	0·62317	−0·96285
0·35	0·16279	0·55888	−0·43191
0·50	0·24174	0·49415	−0·41346
1·00	0·44375	0·32561	−0·27161
2·00	0·66459	0·14139	−0·11795
5·00	0·82018	0·01155	−0·00966
10·00	0·83370	0·00015	−0·00015
12·00	0·83381	0·00000	−0·00003

be the dominant mechanism of heat transfer: the temperature profile through the flow reversal region is extremely close to linear. This gives support for the conduction correction Richardson used [2] for the inner streaming region in his analysis of heat transfer by acoustic streaming alone.

DISCUSSION

The effects of vibrations and oscillations on time-averaged heat or mass transfer have technological importance. Until very recently, it was not possible to compare experimental results with any analysis based upon an acceptable fluid-mechanical representation. This paper presents the first analysis, within the framework of boundary-layer theory, which predicts effects of large magnitude (i.e. changes in heat transfer by a factor of up to 2 or so) from the undisturbed state, and for which there is experimental evidence of changes in flow patterns and of local heat transfer in qualitative agreement.

Table 13d. *Solution of* $F''' - Kf(\lambda E) = 0$; $\lambda = 25$; $\varepsilon = 0{\cdot}9975$ (*Limiting case*, $Re_s \to 0$)

E	F	F'	F''	$f(\lambda E) - 0{\cdot}5$
0·0	0·0	0·0	−12·46864	0·0
0·01	−0·00052	−0·09381	−6·34942	−0·02661
0·02	−0·00168	−0·12899	−0·82066	−0·09129
0·04	−0·00381	−0·05760	7·21326	−0·26952
0·06	−0·00322	0·12909	10·73745	−0·44163
0·08	0·00155	0·34720	10·57931	−0·56027
0·10	0·01048	0·53797	8·27387	−0·61449
0·17	0·06037	0·79027	0·19884	−0·54073
0·24	0·11474	0·75749	−0·44998	−0·49221
0·35	0·19701	0·74699	0·03499	−0·50028
0·50	0·30921	0·74812	−0·00129	−0·49997
1·00	0·68326	0·74809	0·00000	−0·50000
5·00	3·67559	0·74809	0·00000	−0·50000
12·00	8·91215	0·74809	0·00000	−0·50000

The nature and extent of this agreement encourages the hope that the analysis can be extended to reproduce the circumstances of available measurements more precisely. This requires solution of the Navier–Stokes equations directly rather than in their simplified (boundary layer) form: and this involves a large number of boundary values for which iteration is required, together with direct specification of the Grashof number and the cylinder radius (hence some loss of generality), and also modification of the outer boundary conditions to allow for the range of acoustic streaming at small streaming Reynolds numbers. At small streaming Reynolds numbers the effect of the inertia terms in reducing the streaming motion is greatly reduced and it is reasonable to expect a larger influence on heat transfer; this would bring the analytical predictions closer to the experimental data.

There is a possibility of seeking experimental evidence under conditions which more closely approximate those prescribed for the analysis than the experimental data now available. The experiments should be performed by oscillating a cylinder of large diameter at relatively low frequencies—a radius of about 10 cm is suggested, oscillated at 50–100 cps in air, say. The low frequencies are useful in assuring that the streaming Reynolds numbers are large, and that the acoustic wavelength is much larger than the cylinder diameter. The literature already contains some overall heat-transfer data for small cylinders (radius of the order of 1 cm) oscillated vertically and horizontally in this frequency range [14–16], and the data asymptote to expectation from isothermal streaming analysis at large Re_s, but local data are needed for comparison with this analysis.

The use of a large cylinder diameter has the advantages of reducing the value of (a/d) for a given a, and of increasing the Grashof number for a given cylinder temperature. Mechanical oscillation of the cylinder would be required, because it would not be possible at present to produce a standing sound field of uniform intensity at the very high amplitudes required. For observation of local transfer rates it is often more convenient to measure mass transfer of naphthalene or paradichlorobenzene, and some computations were performed for $Pr = 2{\cdot}85$ to correspond to this.

A further extension of the work reported here would involve solution of further pairs of simultaneous ordinary differential equations in the style of the sequence used by Chiang and Kaye in a series representation of the flow and temperature fields away from the bottom stagnation point. Experiments indicate that the "bubble" of reversed flow developed in a vertical sound field closes by about one radian round the cylinder from the bottom stagnation point, and it would be rather gratifying if this could be matched by analysis. However, this requires extensive computer memory if it involves computations through many pairs of equations in the sequence, and our computations with two further pairs of equations suggested that convergence of the series decreases as ε increases.

In more general terms, there are two important considerations relating to future work on the effects of vibrations and oscillations on convective heat transfer. The success of the results reported here, in comparison with experiments, together with that of the analysis based on acoustic streaming by itself [2], encourage the belief that the formulation of the problem is adequate. This formulation is based on the idea that the stready convective motion is created or modified by the Reynolds stresses associated with the oscillating motion. The second consideration is a practical one: with present digital computer speeds and capacities the time required for computation is considerably greater than for more simple, classical problems in boundary layer theory and there is a need for some perceptive analytical procedures which could afford useful results at lesser cost in further applications of the theory.

ACKNOWLEDGEMENTS

The work reported in this paper is part of the research program of heat transfer in unsteady flows of the Aeronautical Research Laboratories, Office of Aerospace Research of the US Air Force. The computation has been supported by NSF Grant GP-4825. This support is gratefully acknowledged.

This work was begun while one of us (G. de V. D.) was Visiting Associate Professor at Brown University, on leave from the University of New South Wales. We are very grateful for the assistance of Mr. J. A. Peterka in the execution of this work.

REFERENCES

1. P. D. RICHARDSON, Effects of sound and vibrations on heat transfer, *Appl. Mech. Rev.* **20**, 201 (1967).
2. P. D. RICHARDSON, Heat transfer from a circular cylinder by acoustic streaming, *J. Fluid Mech.* **30**, 337 (1967).
3. H. SCHLICHTING, *Boundary Layer Theory*, transl. J. KESTIN. McGraw-Hill, New York (1960).
4. J. T. STUART, Double boundary layers in oscillatory viscous flow, *J. Fluid Mech.* **24**, 673 (1966).
5. R. HERMANN, Heat transfer by free convection from horizontal cylinders in diatomic gases, NACA TM 1366 (1954).
6. T. CHIANG and J. KAYE, On laminar free convection

from a horizontal cylinder, Proc. 4th U.S. Natl. Congr. Appl. Mech., 1213 (1962).
7. D. A. SAVILLE and S. W. CHURCHILL, Heat and mass transfer by free convection outside horizontal cylindrical bodies of arbitrary contour, Proc. 5th U.S. Nat. Congr. Appl. Mech., 811 (1966); see also *J. Fluid Mech.* **29**, 391 (1967).
8. S. W. CHURCHILL, The prediction of natural convection, Proc. Third Intl. Heat Trans. Conf., Vol. VI, 15 (1966).
9. P. R. NACHTSHEIM and P. SWIGERT, Satisfaction of asymptotic boundary conditions in numerical solution of systems of non-linear equations of boundary-layer type, NASA TN D-3004 (1965).
10. P. D. RICHARDSON, The effect of vibrations and oscillations on heat transfer from a circular cylinder, USAF Aerospace Res. Labs. Rept. ARL 66-0235 (1966).
11. P. D. RICHARDSON, Influence of sound upon local heat transfer from a cylinder, *J. Acoust. Soc. Am.* **36**, 2323 (1964).
12. R. M. FAND, J. ROOS, R. CHENG and J. KAYE, The local heat transfer coefficient around a heated horizontal cylinder in an intense sound field, *J. Heat Transfer* **84**, 245 (1962).
13. P. D. RICHARDSON, Local details of the influence of a vertical sound field on heat transfer from a circular cylinder, Proc. 3rd Intl. Heat Transfer Conf., vol. 3, p. 71 (1966); *see also* Local effects of horizontal and vertical sound fields on natural convection from a horizontal cylinder, *J. Sound Vibration* **10**, e1 (1969).
14. R. M. FAND and J. KAYE, The influence of vertical vibrations on heat transfer by free convection from a horizontal cylinder, Proc. 2nd International Ht. Trans. Conf. Boulder, Colorado, Paper No. 58 (1961).
15. R. M. FAND and E. M. PEEBLES, A comparison of the influence of mechanical and acoustical vibrations on free convection from a horizontal cylinder, *J. Heat Transfer* **84**, 268 (1962).
16. H. C. LOWE, Heat transfer from a vibrating horizontal tube to air, M. Sc. (Eng.) thesis, University of London (1965).

CONVECTION NATURELLE DANS UN CHAMP SONORE

Résumé—On considère la convection naturelle autour d'un cylindre circulaire horizontal et isotherme placé dans un champ sonore transversal qui se propage dans la direction verticale ou horizontale. Ce problème est traité dans le cadre de la théorie de la couche limite et on a tenu compte de la création ou de la modification du movement permanent convectif par les contraintes de Reynolds associées aux oscillations. Les résultats sont présentés pour un domaine de paramètres exprimant les caractères de la couche limite et les amplitudes des oscillations pour $Pr = 0{,}7$ et 2,85. Les oscillations horizontales accroissent le transfert thermique à la base du cylindre et les oscillations verticales diminuent le transfert thermique local; quand l'intensité des oscillations verticales est assez grande, il se développe une région d'écoulement inversée; les effets correspondants ont été observés expérimentalement.

FREIE KONVEKTION IN EINEM SCHALLFELD UND BEI GROSSEN REYNOLDSZAHLEN

Zusammenfassung—Es wird die freie Konvektion um einen horizontalen isothermen Kreiszylinder betrachtet in Verbindung mit einem transversalen Feld stehender Schallwellen mit vertikaler bzw. horizontaler Ausbreitungsrichtung. Das Problem wird im Rahmen der Grenzschichttheorie behandelt unter Berücksichtigung der Erzeugung oder Veränderung der stationären Konvektionsbewegung durch Reynoldssche Schubspannungen, die in Verbindung mit den Schwingungen auftreten. Die angeführten Ergebnisse umfassen für $Pr = 0{,}7$ und 2,85 einen Bereich von Parametern, die aus Grenzschicht- und Schwingungsgrössen bestehen. Horizontale Schwingungen erhöhen den Wärmeübergang unten am Zylinder, vertikale Schwingungen vermindern den örtlichen Wärmeübergang; wenn die Intensität der vertikalen Schwingungen gross genug ist, bildet sich ein Gebiet mit Strömungsumkehr aus; entsprechende Effekte wurden in den Experimenten beobachtet.

ВЛИЯНИЕ АКУСТИЧЕСКОГО ПОЛЯ НА СВОБОДНУЮ КОНВЕКЦИЮ

Аннотация—Рассматривается естественная конвекция вблизи горизонтального кругового изотермического цилиндра совместно с поперечным стоячим акустическим полем, распространяющимся в вертикальном или горизонтальном направлении. Задача рассматривается в рамках теории пограничного слоя с учетом возникновения или изменения конвективного стационарног движения в результате напряжений Рейнольдса, вызванных колебаниями. Представлены результаты для диапазона изменения параметров пограничного слоя и значений колебаний при $Pr = 0{,}7$ и 2,85.

Горизонтальные колебания усиливают теплообмен у основания цилиндра, а вертикальные уменьшают локальный теплообмен.

При достаточно большой интенсивности вертикальных колебаний развивается область обратного течения. Соответствующие эффекты наблюдались экспериментально.